Energy Efficient Control Technique for SRM Drives

Maged N. F. Nashed
Department of Power Electronic and Energy Conversion
Electronics Research Institute, El Tahrir st., Cairo, Egypt
maged@eri.sci.eg

Abstract—**This paper describes modeling and machine independent method to minimize the energy consumption of a speed controlled Switched Reluctance Motor (SRM). The method for modeling depends on the mathematical models of SRM under an a-b-c stationary frame and a d-q synchronous frame. The control strategy is to vary the dutycycle of the applied current regulator in order to obtain the desired speed quickly. When operating in steady state vary the turn-on angle (θ_{on}) of the phase-voltage to minimize the energy consumption. The power flow is measured in the DC part and used to control the turn-on angle. Simulations the system on a 6/4 pole SRM justify the algorithm. Measurements on load systems show it is possible to minimize the energy consumption on-line in a speed controlled SRM without loosing the dynamic performance. The algorithm is fully applicable to other SRM at other power levels or with other pole configurations.**

Keywords: Switched reluctance motor, current regulator, inverter with drive and Position and Speed sensors.

I. Introduction

SRM experiences a revival due to improvements in power devices, low-cost micro-controllers and computer-aided design tools. In comparison with AC-machines or commutated DC machines, the SRM is less expensive in production and design. It is also very suitable for high speed applications. The disadvantages are the need of position feedback sensors and the produced torque-ripple, which may cause acoustic noise.

An important factor in electrical drives is high efficiency and low cost. Some papers have considered energy optimized control of AC-machines like minimizing the energy consumption by adjusting the rotor slip frequency [1], which gives a high dynamic performance. Another strategy is to minimize the energy consumption by measuring the DC-link current and voltage and in steady-state adjusting the voltage/frequency ratio [2]. Very few papers have considered such strategies for SRM but this paper will deal with a new developed control strategy based on a DC-link current measurement.

The SRM is usually voltage controlled or current controlled. Voltage control means applying a phase voltage consisting of a chopped DC-voltage with constant dutycycle (D). The dutycycle is thus the control signal and no current control loop is used. In current control, the phase current is compared to a reference current and the phase voltage is controlled by a hysteresis control. The reference current is then the control signal. Apart from the dutycycle (or the reference current) and the angular speed, two other parameters determine the electromechanical torque production. These are the turn-on angle (θ_{on}) and the turn-off angle (θ_{off}) which are angles defined in relation to the rotor position of the SRM**.** A traditional control of the firing angles is presented in [3, 4]. The firing angles are moved in steps dependent on the speed and the same firing angles are then used for a wide speed range. This control strategy is referred as mode-shift control. Another paper [5] has treated optimum control of the firing angles, e.g. minimum power consumption at constant speed and shaft torque. These were experimentally achieved and stored for later use in a microcontroller. The limit of this method is that the optimum firing angles are application specific, and therefore can change with different load conditions. A third paper [6, 7] optimize the torque-ripple by adjusting the turn-off angle which in many cases will have much less effect compared with an adjustment of the turn-on angle. A non-application specific power minimization method is proposed in this paper based on turn-on angle control.

In this paper, the models of a three-phase SRM under an a-b-c stationary frame and a d-q synchronous frame are presented. The torque equation is derived according to the real self-inductances of the SRM. Next, the new energy optimizing strategy will be explained and a detailed implementation given. Finally, Simulation results will be shown for this model.

II. System Description and Modeling

1. System Description

The block diagram of SRM drive system is shown in Fig. 1. This system consists of four major parts: a motor, a current-regulated converter, a controller, and inverter with drive. First, the controller computes the speed error and then executes the control algorithm. Next, the controller determines and outputs the current commands to the current-regulated converter. The current-regulated converter controls the three phase currents to follow the current commands.

2. Stationary frame model

The SRM is a nonlinear system. The self-inductance of the motor is related to the position of the rotor. We can assume that each phase's self-inductance is not related to its phase current The flux linkage of the motor, therefore, can be expressed as, [8]:

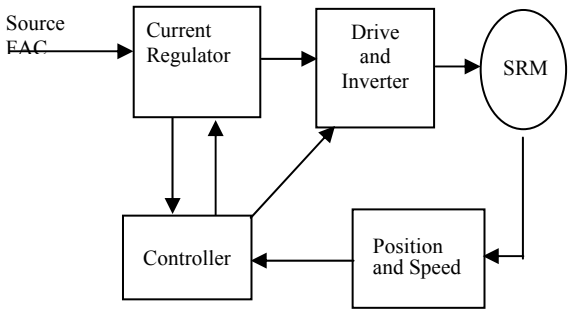

Fig. 1, Block Diagram of SRM System.

$$\lambda_j(\theta_e, i_j) = L_j(\theta_e) i_j \qquad j = a, b, c \tag{1}$$

where λ_j is the flux linkage of each (a, b, c) phase,
L_j is each phase's self-inductance,
i_j is each phase's current, and
θ_e is the electrical rotating angle.

The self-inductance of different phases has the same shape but shifts a 120° electrical phase angle. The dynamic equation of each phase voltage is

$$\begin{aligned} v_j(\theta_e) &= R_s i_j + \frac{d}{dt}\lambda_j(\theta_e, i_j) \\ &= R_s i_j + L_j(\theta_e)\frac{d}{dt} i_j + i_j \frac{dL_j(\theta_e)}{d\theta_e}\omega_r \end{aligned} \tag{2}$$

where v_j is the phase voltage, R_s is the phase resistance, and ω_r is the electrical rotating speed. The torque of the motor is

$$\begin{aligned} T_e(\theta_e, i_j) &= N_r \sum_{j=a,b,c} \frac{\partial}{\partial\theta_e}\int_0^{i_j} L_j(\theta_e) i_j di_j \\ &= N_r\left(\frac{1}{2} i_a^2 \frac{dL_a(\theta_e)}{d\theta_e} + \frac{1}{2} i_b^2 \frac{dL_b(\theta_e)}{d\theta_e} + \frac{1}{2} i_c^2 \frac{dL_c(\theta_e)}{d\theta_e}\right) \end{aligned} \tag{3}$$

Where: N_r is the number of rotor teeth, L_a, L_b, and L_c are the a, b, c phases' self-inductances. The electrical speed of the motor is

$$\frac{d}{dt}\frac{\omega_r}{N_r} = \frac{1}{J_m}\left(T_e - B_m \omega_r \frac{1}{N_r} - T_l\right) \tag{4}$$

Where ω_r is the electrical speed, J_m is the inertia, B_m is the viscous coefficient, and T_l is the external load.

3 *Synchronous frame model*

The relationship transformation between d-q axis and a-b-c axis can be expressed as

$$\begin{bmatrix} f_q \\ f_d \\ f_0 \end{bmatrix} = \begin{bmatrix} \cos\theta_e & \cos(\theta_e - 120^0) & \cos(\theta_e + 120^0) \\ \sin\theta_e & \sin(\theta_e - 120^0) & \sin(\theta_e + 120^0) \\ 0.5 & 0.5 & 0.5 \end{bmatrix} \begin{bmatrix} f_a \\ f_b \\ f_c \end{bmatrix} \tag{5}$$
$$= T(\theta) f_{abc}$$

Where f_q, f_d, and f_o are the synchronous of q-axis, d-axis and zero-sequence of voltages or currents, T is the a-b-c to d-q axis transformation, and f_a, f_b, and f_c are the stationary a, b, and c-axis voltages or currents. The synchronous d-q axis voltage equations are:

$$v_q = R_s i_q + \omega_r \lambda_d + p\lambda_q \tag{6}$$

$$v_d = R_s i_d - \omega_r \lambda_q + p\lambda_d \tag{7}$$

Where v_d i_d, v_q and i_q are the d-axis and q-axis for voltage and current, λ_d and λ_q are the d-axis and q-axis of flux. The torque of the motor is:

$$T_e = \frac{3}{2} N_r(\lambda_d i_q - \lambda_q i_d) \tag{8}$$

III. Torque Pulsation Reduction

Fig. 2 shows the ideal self-inductance waveforms of a SRM. Each self-inductance increases/decreases linearly when its related stator and rotor teeth move closer or farther away. The self-inductance is maintained at a constant when its related stator and rotor teeth are aligned. According to the self-inductance waveforms, we can obtain the ideal phase current commands, which can produce maximum average torque and minimum torque pulsations. The current command of each phase is a square wave with a 1/3 duty cycle. Each phase's current is injected into the motor when its related self-inductance is increased. By summing-up the three-phase torque, we can obtain the smoothing torque. The real self-inductance can be approximately expressed as [9, 10]:

$$L_a(\theta_e) = L_{ls} + L_A - L_{Bl}\cos(\theta_e) + \sum_{n=2,3,\ldots}^{N} L_{Bn}\cos(n\theta_e) \tag{9}$$

$$L_b(\theta_e) = L_{ls} + L_A - L_{Bl}\cos(\theta_e - 120^0) + \sum_{n=2,3,\ldots}^{N} L_{Bn}\cos[n(\theta_e - 120^0)]$$

$$L_c(\theta_e) = L_{ls} + L_A - L_{Bl}\cos(\theta_e + 120^0) + \sum_{n=2,3,\ldots}^{N} L_{Bn}\cos[n(\theta_e + 120^0)]$$

And $$\theta_e = N_r \theta_{rm} \tag{10}$$

Where L_{ls} is the leakage inductance, L_A, L_{B1}, L_{Bn} are the parameters of the self-inductance, and θ_{rm} is the mechanical shaft angle.

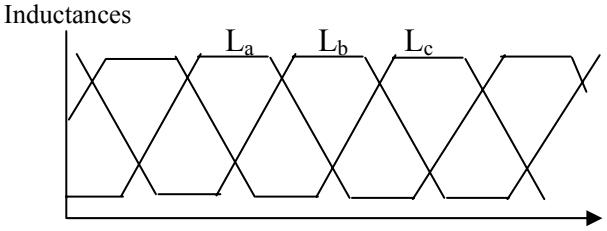

Fig. 2, Waveforms of the SRM ideal inductances.

To calculate the torque pulsation select only the fundamental and DC components as the self-inductance. The harmonics of the self-inductance in equation (9) are neglected because they are very small when compared with the fundamental component [4]. Then, the approximate inductances are

$$
\begin{aligned}
L'_a(\theta) &\cong L_{ls} + L_A - L_{B1}\cos(\theta_e) \\
L'_b(\theta) &\cong L_{ls} + L_A - L_{B1}\cos(\theta_e - 120^0) \\
L'_c(\theta) &\cong L_{ls} + L_A - L_{B1}\cos(\theta_e + 120^0)
\end{aligned} \qquad (11)
$$

Where L'_a, L'_b, L'_c, are approximate values of the self-inductances in the a-b-c stationary frame. The approximate values of the self-inductances in the d-q synchronous frame are:

$$
\begin{bmatrix} L'_q & 0 & 0 \\ 0 & L'_d & 0 \\ 0 & 0 & L'_0 \end{bmatrix} = T(\theta)^{-1} \begin{bmatrix} L'_a(\theta_e) & 0 & 0 \\ 0 & L'_b(\theta_e) & 0 \\ 0 & 0 & L'_c(\theta_e) \end{bmatrix} T(\theta) \qquad (12)
$$

$$
= \begin{bmatrix} L_{ls} + L_A - L_{Bl} & 0 & 0 \\ 0 & L_{ls} + L_A + L_{Bl} & 0 \\ 0 & 0 & L_{ls} \end{bmatrix}
$$

Where L'_d and L'_q are the approximate values of the d-q axis inductances and constant values. If the current commands are sinusoidal waveforms, the mutual inductances have to be considered. Then, the L'_d and L'_q of the equation (12) are multiplied by 1.5. The d-q axis currents (i_d and i_q), which are orthogonal, can be defined as

$$
\begin{aligned}
i_d &= i_s \cos\delta \\
i_q &= i_s \sin\delta
\end{aligned} \qquad (13)
$$

Where i_s is the amplitude of the current vector $= \sqrt{i_d^2 + i_q^2}$,

δ is the phase angle of the current vector = $\tan^{-1}(i_q/i_d)$.

The torque can be derived from equation (8), and it is expressed as:

$$
T_e = \frac{3}{2} N_r (L'_d - L'_q) i_d i_q \qquad (14)
$$

If we choose $\delta = 45^0$, then the torque ratio T_e/i_s has a maximum value, and this control is called "maximum torque" control. On the other hand, if we maintain i_d as a constant, and only adjust i_q, then the torque is proportional to i_q. This is called "field oriented" control. The phase currents i_a, i_b, i_c can be computed according to the coordinate transformation:

$$
\begin{bmatrix} i_a \\ i_b \\ i_c \end{bmatrix} = T(\theta) \begin{bmatrix} i_q \\ i_d \\ i_0 \end{bmatrix} \qquad (15)
$$

The current command waveforms i_a, i_b, i_c are sinusoidal waveforms in spite of maximum torque or field oriented controls. By suitably adjusting the amplitude, frequency, and phase, the torque can be effectively controlled. The torque pulsation due to the harmonics of the self-inductances is neglected here. The reason is that the harmonics of each phase self-inductance are much smaller when compared with the fundamental sinusoidal component of the self-inductance. If we consider both the average torque and the torque pulsation, then

$$
T_e = \frac{3}{2} N_r \left[(2L_{B1}) i_d i_q + \sum_{n=2,3,\ldots}^{N} (2nL_{Bn}) i_{dn} i_{qn} \right] \qquad (16)
$$

Where i_{dn} and i_{qn} are the equivalent d-q axis currents with the shaft angle $n\theta_e$ and the shaft rotating speed $n\omega_e$ because they are related to the nth harmonics of the self-inductances.

IV. Energy Optimizing Control Strategy

In order to get an optimized operating point at all speeds and all loads it is necessary to use the turn-on and turn-off angles as control parameters. The proposed strategy to minimize the power consumption is based on the principle shown in Fig. 3**.**

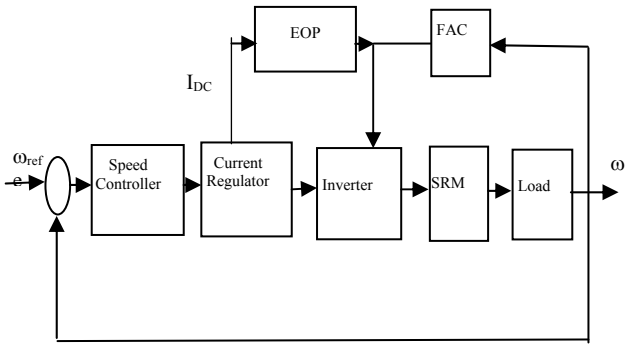

Fig. 3, Proposed energy optimizing control of SRM with floating angle control.

Instead of measuring and using the RMS phase current for an energy optimization, the current Regulator I_{DC} is used. I_{DC} reflects the active power fed into the inverter. In order to minimize the total power consumption which includes both the inverter and the SRM, the current regulator is measured and voltage is assumed to be constant. The Floating Angle Control (FAC) in Fig. 3 is following a 1st order function of speed determined by the optimum θ_{on} and θ_{off} at low and high speed. The θ_{on} and θ_{off} used in the FAC-control are given by:

$$
\begin{aligned}
n < n_3 \quad & \theta_{on} = 15^0 \\
n > n_3 \quad & \theta_{on} = 15^0 - \frac{(n - n_3)}{3000} * 20 \\
n < n_2 \quad & \theta_{off} = 42^0 \\
n > n_2 \quad & \theta_{off} = 42^0 - \frac{(n - n_2)}{3000} * 20
\end{aligned} \qquad (17)
$$

$\theta_{on,min} = -15^0$ (minimum turn-on angle)
$\theta_{off,min} = 30^0$ (minimum turn-off angle)
where: n = rotational speed,
θ_{on} = turn-on angle
θ_{0ff} =turn-off angle

The functions for the firing angles are explained by simulations. They represent the firing angles which provide almost maximum efficiency. Fig. 4. shows θ_{on} and θ_{off} for the FAC as a function of speed.

The control strategy of the energy optimizer is then:

1- The speed controller assures the wanted speed by varying the duty-cycle at an initial turn-on angle and a fixed turn-off angle, which is controlled by the FAC.
2- In steady-state the load torque remains constant and the power flow is measured in the current regulator (V_{DC}, I_{DC}) by the Energy Optimizing Program (EOP)

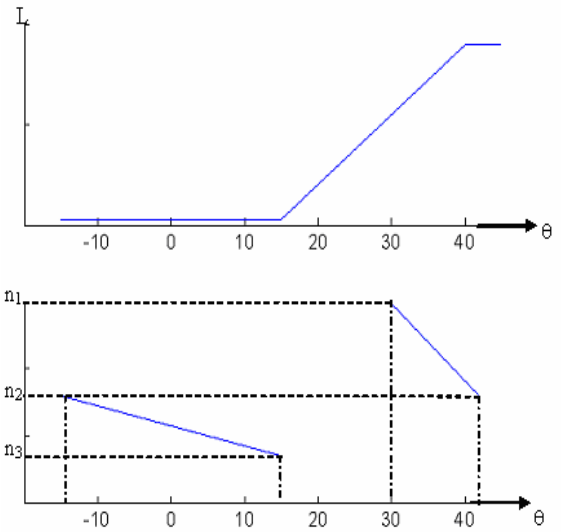

Fig. 4, Floating Angle Control (FAC)- turn-on and turn-off angles. n_1=7000rpm, n_2=4000rpm, n_3=1400rpm.

3- The turn-on angle is changed $\Delta\theta_{on}$ in either direction.
4- The speed controller changes the dutycycle to reassure the desired speed.
5- When steady-state is reached again, a new set of (θ_{on}, D) are obtained which exactly produce the needed torque and gives a new power flow.
6- If the power flow has decreased, θ_{on} is moved further in the same direction (the sign of $\Delta\theta_{on}$ is unchanged). If the power flow has increased, the sign of $\Delta\theta_{on}$ is changed.

This is repeated until the change in power flow is too small to encourage any change in angle and the turn-on angle will alternate between two or three angles, which all give the highest efficiency. Fig. 5 shows a flow chart of EOP. The energy optimization principle is illustrated in Fig. 6 by simulations.

V. SRM Simulation System and Results.

The parameters used to simulate the 6/4 SRM were previously obtained by experiment measure. The SRM nonlinear dynamic model is completed on Matlab/Simulink environment, [7, 8]. Fig.7 shows the simulation diagram used for the SRM model. Fig. 8 shows the relation between phase Current data versus flux and rotor position for SRM. Fig. 9 shows static torque in rotor position at different values of stator current. The phase of voltage, torque, current and rotor position are shown in Fig. 10, While The effect of the change of θ_{off} on the Current, phase voltage and torque are shown in Fig. 11.

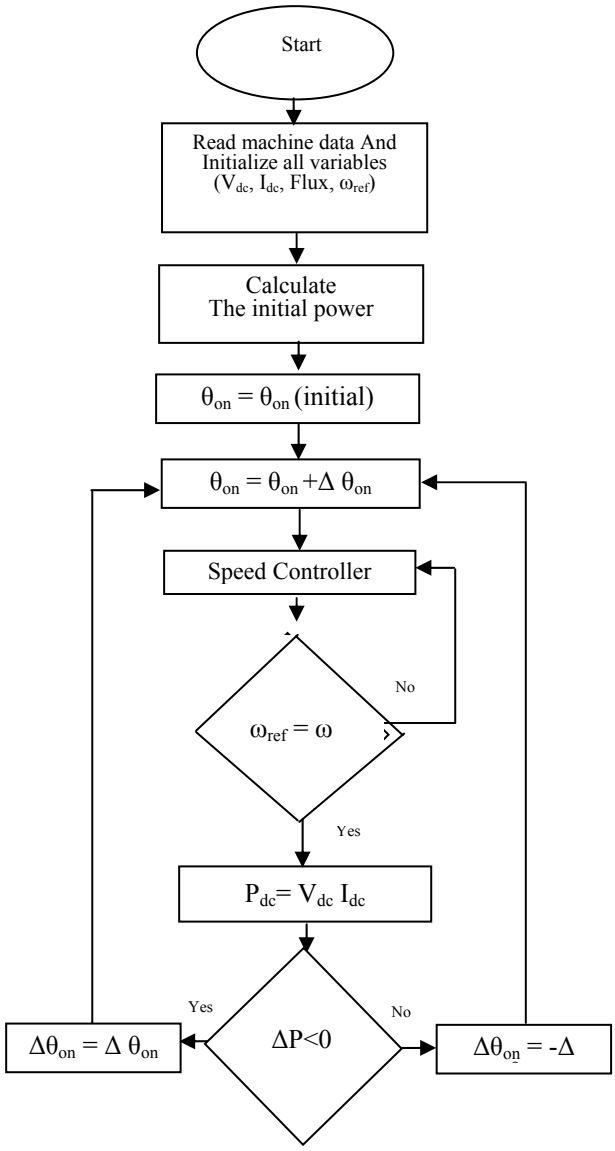

Fig. 5. Flow chart for proposed EOP control of SRM.

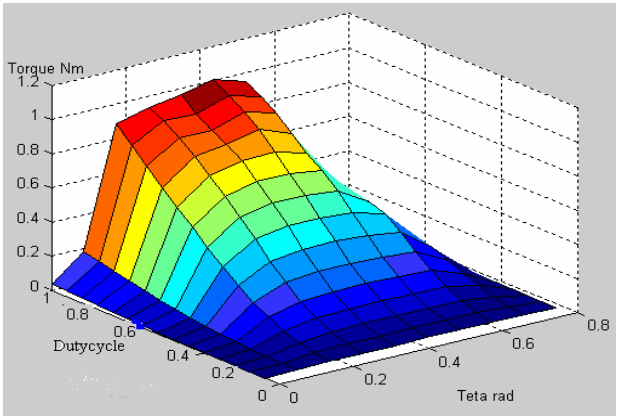

Fig. 6. Simulated (θ_{on}, D) trajectory for constant speed n = 2000 rpm

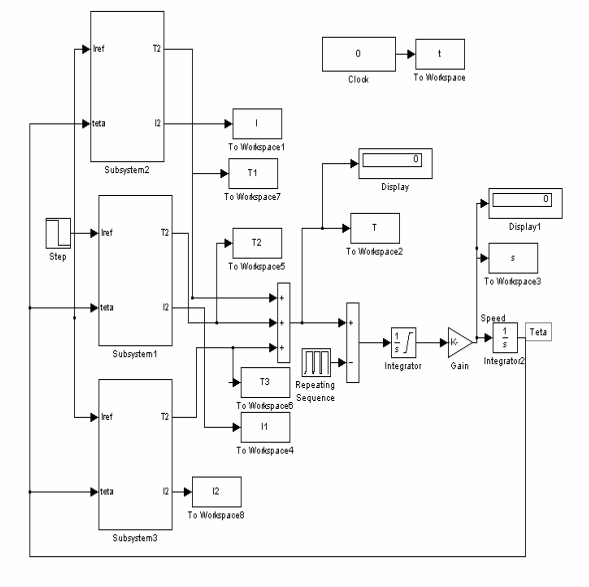

Fig. 7. Simulation blocks for SRM model.

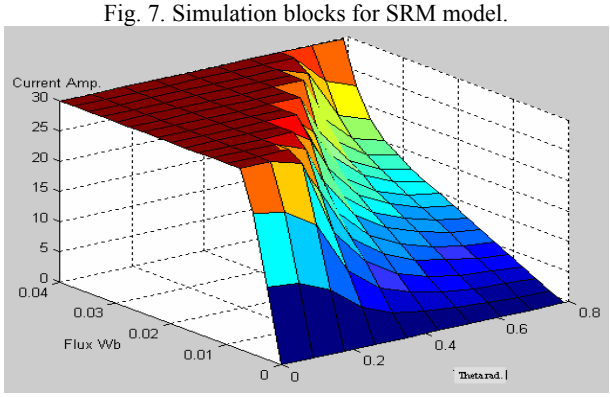

Fig. 8, Phase Current data versus flux and rotor position for SRM.

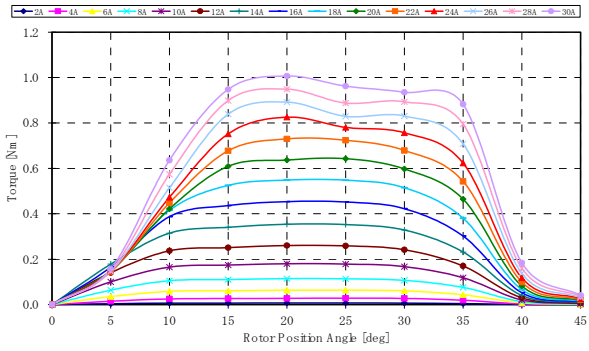

Fig. 9, Relationship between rotor position angle and torque.

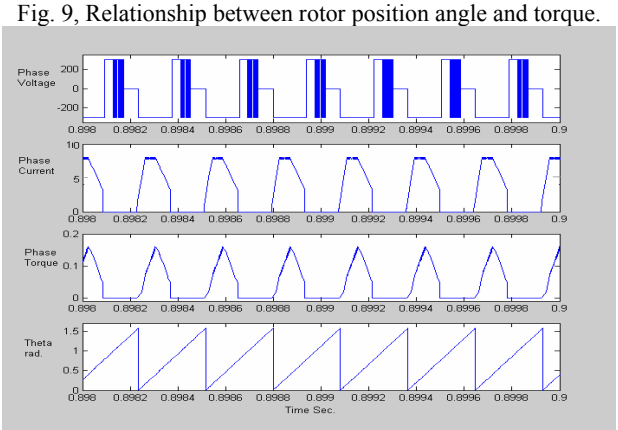

Fig. 10, Phase of voltage, current, torque and rotor position.

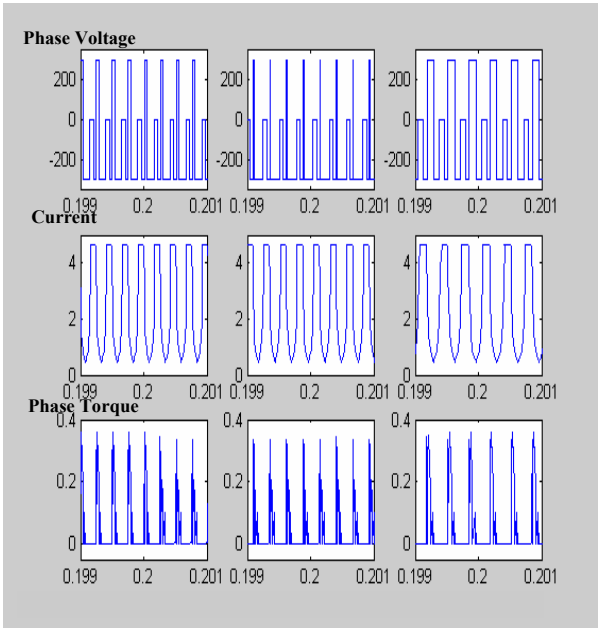

Fig. 11, Effect of the change of θ_{off} on the current, phase voltage and phase torque

Fig. 12 shows the average of phase and total torque and the value of average total torque = 0.1434 Nm, While the value of average phase torque = 0.1202 Nm. The simulation result of speed, torque and current for SRM are shown in Fig. 13. Fig. 14 shows the speed, current, and torque at change of the reference speed without control and with control.

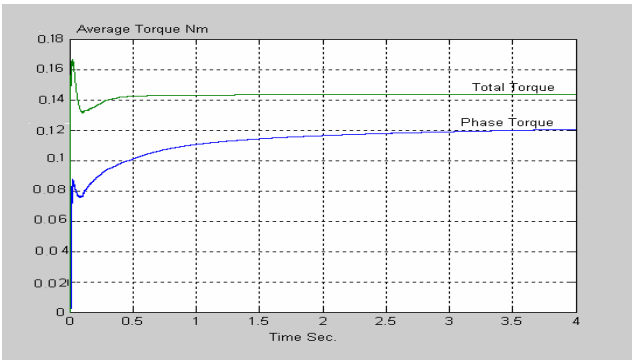

Fig. 12, Average total torque and phase torque.

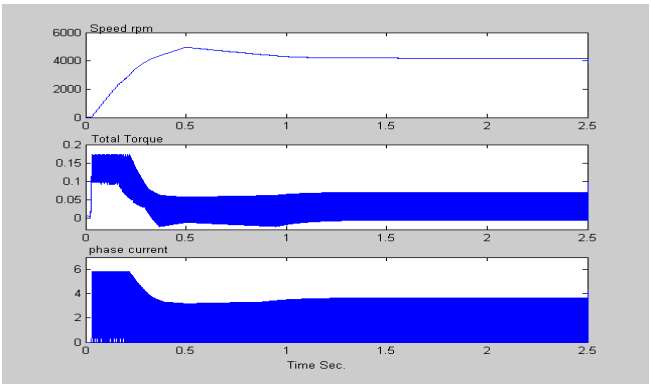

Fig. 13, Simulation result of Speed, torque and current for SRM.

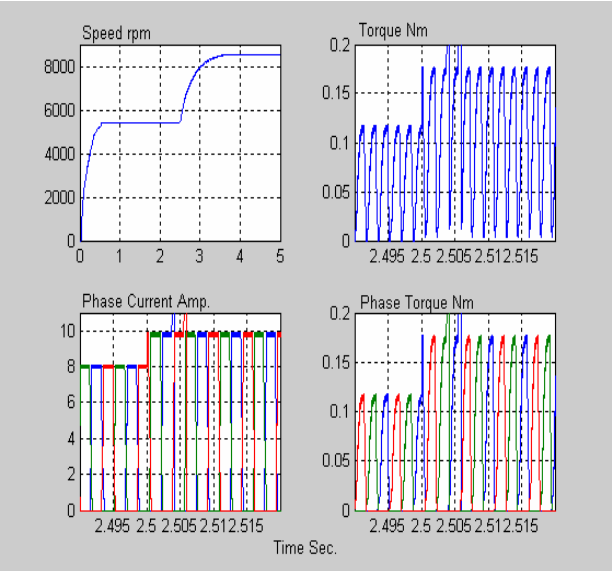

(a) Without control.

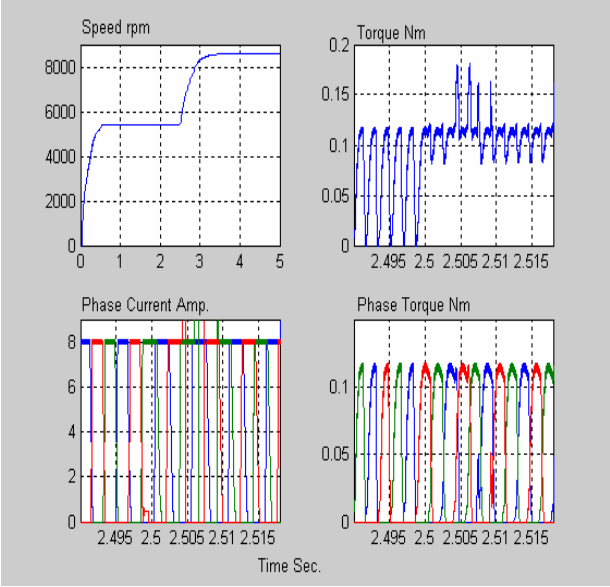

(b) With control

Fig. 14, Speed, current, and torque at change of the reference speed.

V. CONCLUSION

A method approach to modeling depend on the mathematical modeled of SRM under an a-b-c stationary frame and a d-q synchronous frame and optimizing the power consumption of a voltage controlled SRM when it runs at steady-state has been introduced. It requires regular measurement of the power flow in the current regulator and control of the turn-on angle θ_{on}, and tum-off angle θ_{off} as a function of speed. An intemal control loop with a speed controller, which uses the dutycycle of the applied phase voltage as control parameter, assures the desired speed, regardless of the turn-on angle. The algorithm used for energy optimization is applicable to any SRM and the strategy takes the characteristics of the converter into account.

APPENDIX

Motor data:
Number of stator/ rotor Poles: 6/4
Maximum Speed: 8000 rpm
Excitation Current : 2-30 Amps
Rated Torque : max 1 Nm
Aligned Phase Inductance : 2.2 mH
Unaligned Phase Inductance: 0.27 mH
Number of windings/poles : 24 turns/poles

REFERENCE

[1] A. Adnanes, R. Nilsen, R. Loken and L. Norum, “Efficiency Analysis of Electric Vehicles, with Emphasis on Efficiency Optimized Excitation”, Proceedings of IEEE International Electrical Vehicle Symposium, 2003, pp. 455-462.

[2] J. Holtz “Sensorless Speed and Position Control of IM”, The 27th Annual Conference of the IEEE Industrial Electronics Society, IECON'01, Vol. 3, 29 Nov-2 Dec 2001, Colorado, USA, pp. 1547-1562.

[3] T. Miller, C. Cossar, and D. Anderson, "A New Control IC for SRM Drives", 5th Inter. Conf. on Electrical Machines and Drives, IEE, 1991, London, pp. 331-33.5.

[4] R. Becerra, M. Ehsani, and T. Miller, "Commutation of SRM", IEEE Applied Power Electronics Conference and Exposition, 1991. APEC'91, Sixth Annual, 10-15 Mar., 1991, pp. 181-187.

[5] H. Zhang, J. Zhang and R. Gao, “A Novel Method of Phase Current Compensation for SRM System Based on Finite Element”, Journal of Computers, Vol. 4, No. 10, Oct. 2009, pp. 1064-1071.

[6] R. Orthmann, and H. Schoner, “Turn-off Angle Control of SRM for Optimal Torque Output", Proceeding of European Power Electronics Association of EPE '93, Vol. 6, 1993, pp. 20-25.

[7] M. Nashed, K. Ohyama, K. Aso, H. Fujii, and H. Uehara “Automatic Turn-off Angle Control for High Speed SRM Drives” IEEE International Symposium on Industrial Electronics ISIE 2006, July 9-12, 2006, Montréal, Québec, Canada, pp 2152-2157.

[8] K. Ohyama, M. Nashed, K. Aso, H. Fujii, and H. Uehara “Design Using Finite Element Analysis of SRM for Electric Vehicle” The Korean Institute of Power Electronics (KIPE), Journal of Power Electronics, Vol.6, No.2, Korea, Ap.2006 pp 163-171.

[9] M. Nashed “Simulation and Experimental of Bi-Direction Converter With Input PFC on SRM System” The Korean Institute of Power Electronics (KIPE), Journal of Power Electronics, Vol. 6, No. 2, Korea, April, 2006 pp 121-130.

[10] I. Husain and M. Ehsani, "Rotor Position Sensing in SRM Drives by Measuring Mutually Induced Voltages," IEEE Trans. Ind. Application, Vol. 30, No. 3, May/June 1994, pp. 422-429.